Egypt. J. Chem. **Vol. 65,** No. SI:13B pp. 321 - 330 (2022)

Egyptian Journal of Chemistry

http://ejchem.journals.ekb.eg/

Determination Of Refractive Indices Of Heavy Metal Ions Solutions To Evaluate Their Concentrations

Haiam Fahmy, Abeer Salah*, and Gamal Abdel Fattah

Laser Sciences and Interactions department, National Institute of Laser Enhanced Sciences, Cairo University, Cairo 12613, Egypt.

Abstract

Surface plasmon resonance (SPR) sensors have advantages of tracing heavy metal ions content and environmental monitoring. In this work, a surface plasmon resonance structure was built. it was based on Kretschmann structure which is cost-effective. The sensing layer were gold thin film deposited by sputtering technique. The resonance angles (θ_{SPR}) of heavy metal ions Pb^{+2}, Zn^{+2} and Cd^{+2} were shifted to higher values with increasing their content. Complex refractive indices of metal ions were calculated. The real and imaginary parts of refractive indices of heavy metal ions were increased while increasing their concentrations. Data curve fitting yields calculated θ_{SPR} for any unknown concentration of heavy metal ions, also the performance factors were determined which predict the proper use of SPR sensor for different metal ions detection.

Keywords: Surface Plasmon Resonance; Kretschmann configuration; Heavy metal ions; sensor performance; gold thin film; optical properties

1. Introduction

Surface plasmon resonance SPR biosensors showed significance over conventional sensors, which included refractive index sensitivity, fast sensor reaction, real-time detection, and a label-free approach. Moreover, SPR sensors have great other applications in environmental tracking, security, scientific diagnostics, food safety and SPR imaging generation, hence SPR has gained vast momentum with growing of clinical publications [1]–[4].

SPR excitation typically requires high angular momentum for aquatic solution detection. Therefore, a coupling component is required in many designs to ensure the incidence of a large angle at the metal-dielectric interface [5]. The coupling method which lies between light and metal film/dielectric contact is the key component in SPR based–systems. It occurs via grating [6], waveguide, optical fiber and prism couplers which optically excite surface plasmons. Different approaches have been used for measuring SPR as wave length interrogation[7], angular interrogation[8], intensity interrogation[9], phase interrogation[7]. Although other detection techniques are high sensitive but as expensive as atomic absorption spectrometry, inductively coupled plasma mass spectrometry (ICPMS); these instruments are stationary and have complex operation[10]. Researchers studied the SPR based on fiber optics [11] and SPR sensors using smartphone for the portable use [12]. Wavelength modulation and angular modulation are the most common methods [13] [14] where the latter includes measuring the incident angle of light compared to the surface of the prism.

Surface plasmon resonance can be used for heavy metal ions detection, heavy metals are considered harmful to the environment and organisms [13]. An excess of cadmium and mercury in humans can cause damage to liver and several organ failure, respectively [15]. In addition to, several hazardous effects of lead to humans which transferred through food, air, and water. Excess intake of lead caused incurable blood infections and disorder of the nervous system [2] [16]. SPR sensor is attractive simple and cost-effective method for heavy metal detections.

For SPR generation, the incident light must be in a transverse magnetic mode as the electric field is perpendicular to the metal thin film; under the condition of total internal reflection, surface plasmon was generated by the evanescent wave at the metal and dielectric interface. [17] , the propagation constant of the incident light k_x must be equal to wave vector of surface plasmon k_{sp} for the surface plasmon excitation to occur, the resonance condition is given by:

$$k_x = k_{sp} \quad (1)$$

$$\frac{\omega}{c} n_{pr} \sin\theta_{SPR} = \frac{\omega}{c} \sqrt{\frac{n_m^2 n_s^2}{n_m^2 + n_s^2}} \quad (2)$$

*Corresponding author e-mail: abeersalah@niles.edu.eg.; (Abeer Salah).
Receive Date: 03 March 2022, Revise Date: 27 July 2022, Accept Date: 13 September 2022
DOI: 10.21608/EJCHEM.2022.125172.5569

Hence, the refractive index of the sample is given by [18] :

$$n_s = \sqrt{\frac{n_m^2 n_{pr}^2 \sin\theta_{SPR}^2}{n_m^2 - n_{pr}^2 \sin\theta_{SPR}^2}} \qquad (3)$$

Where n_{pr}, $n_{m,}$ and n_s are refractive indices of prism, gold layer, and sample, respectively. ω is the angular frequency of light. c is the speed of light.

In this article, simple SPR sensor is built based on Kretchmann structure. The SPR angle (θ_{SPR}) and the optical properties for the heavy metal ions with different concentrations are determined and investigated. Also, θ_{SPR} and other parameters were computed according to curve fitting analysis for unknown concentrations. In addition, sensor performance for heavy metal ion detection is discussed.

2 Experimental

2.1 Materials

Gold layers are deposited on glass substrates (25.4 × 76.2 mm) with thickness 1-1.2mm with 240s deposition time by sputtering (K550 sputter coater, England). The thickness of gold layer was measured after deposition by electron interference microscope and the average value was 33.5 nm.

The matching immersion oil was used to contact the Au film to the prism; Prism Dimensions were (diameter 4.9 cm and height of 1.7 cm) and Prism refractive index is 1.518. The prism was used to couple p-polarized light with a thin metal film for excitation of surface plasmons. A cell, for holding metal solutions, was constructed from glass. One cell side was internally coated with gold film with thickness 33.5 nm. The cell was in contact with prism through the matching oil. There was no inlet and outlet as in the flow cell. The cell was washed by double distilled water after each run of measuring SPR curves.

The three different salts of metals were lead nitrate [Pb $(No_3)_2$], Zinc nitrate [Zn $(No_3)_2.6H_2o$] and, Cadmium nitrate [Cd $(No_3)_2.4H_2O$] were used as the source of Lead, Zinc and Cadmium stock solutions respectively. 1000 ppm stock solutions were prepared from these salts, and then diluted to 100, 250, 500, 750, 850, and 950 ppm. All the required solutions were prepared with analytical reagents and double-distilled water.

2.2 Surface plasmon resonance detection

The experimental set up was based on Kretschmann arrangement [19]. The optical system consisted of a He-Ne laser, a glass prism which was mounted on the rotational stage, a polarizer (p-polarised light), and an optical chopper (SR 540) as seen in Fig.1. Gold thin film deposited on one side of glass substrate and the other side was in contact to the prism by matching oil. The glass / metal interface was illuminated with He-Ne laser (**λ** =632.8 nm**,** 5 mW). The reflected intensity was measured as a function of the incident angle; a conservation of energy and wave vector simultaneously were satisfied, a dip in light intensity is observed at the resonance angle (θ_{SPR}). The reflected beam was collected by a large area solar cell (Si) detector and then amplified via a lock-in amplifier (SR 530). From SPR spectrum; the resonance angle θ_{SPR} could be determined. Hence, refractive indices calculations were done.

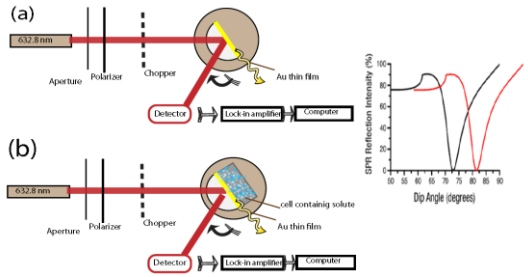

Fig. 1 Experimental set up for achieving SPR (a) in Air, (b) in metal ion solutions.

The solutions of heavy metal salts were prepared by different concentrations from 100 to 1000 ppm and placed in the sample cell. The solution was in contact to the Au films inside the cell as seen in Fig.1b

Different parameters were determined from spr curves as the resonance angle θ_{SPR}, the minimum value of reflected intensity $I_{min.}$, maximum reflected intensity I_{max}, and the angle ($\theta_{max.}$) at which the reflected intensity is of maximum value. The refractive indices were calculated based on the investigated surface plasmon resonance analysis for different metal ions solution.

2.3 Sensor performance parameters

Performance parameters [20],26] of SPR sensor as sensitivity (S), detection accuracy (D.A) and quality factor (Q.F) were calculated and analyzed as a function of metal ion concentrations. Performance of SPR sensors could be deduced based on the three mentioned parameters, where the sensitivity is the ratio of the change in the SPR angle to the change in the refractive index. S measures the ability of sensing the change in refractive index of sensing medium due to the molecules absorption.

$$S = \frac{\Delta\theta_{SPR}}{\Delta n} \qquad (4)$$

The detection accuracy : is the ability of monitor the minimum change in the refractive index of the sensing medium. It is measured as the change in the resonance angle to the full width at half maximum FWHM.

$$D.A = \frac{\Delta\theta_{SPR}}{FWHM} \qquad (5)$$

Quality factor is the quality of the sensor. It is the ratio of the sensitivity (S) to the FWHM. The qualty factor depends on $\Delta\theta_{SPR}, FWHM, \Delta n$. It is important factor to qulaify the overall sensor performance with respect to the measured parmeters.

$$Q.F=\frac{S}{FWHM} \quad (6)$$

Where $\Delta\theta_{SPR}$ is the shift in SPR angle of salt with respect to that of water, FWHM is the width at half maximum of SPR curve and I_{min} is the minimum reflected intensity.

limit of detection (LOD) measures the lowest concentration of ions that the sensor can detect. it can be evaluated by the following equation:

$$LOD= \Delta\theta/S \quad (7)$$

where $\Delta\theta=0.5^o$ is the minmum step of angle measurement and S is the senstivity.

3 Results and discussions

3.1 Surface plasmon resonance of metallic salt solutions

SPR measurements had been carried out by measuring the reflected p-polarized He-Ne laser intensity (632.8 nm, 5 mW) as a function of the incident angle as discussed in section 2.2, A gold layer was deposited on one side of the glass substrate and the other side are in contact to the prism by matching oil. Prior to metal salt measurements, we investigated the SPR for deposited gold in glass substrate and in the designed cell. The reflected intensity as a function of the incident angle was performed as shown on Fig.2. The SPR curves were the same for the two deposited layers which confirm the stability of the sensing and good quality of the prepared gold films.

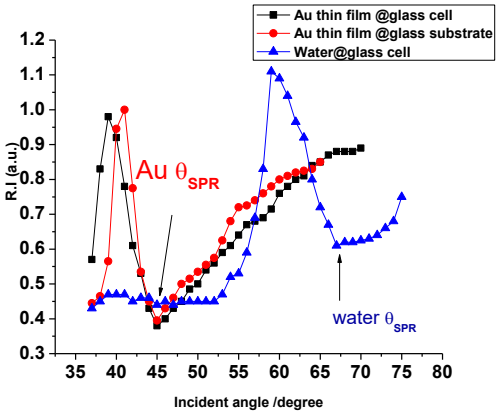

Fig. 2 SPR curves for gold layer on glass substrate, gold layer on the inside wall of the empty sample cell and cell filled with water.

SPR measurements were investigated with double distilled water in constructed cell as seen in Fig. 2. From the resonance angle, the refractive indices of prism, gold and using equation 3, the calculated refractive index of distilled water n_w =1.29448131+0.00981178i.

The reflected intensity was studied as a function of the incident angle for (Pb^{+2}, Cd^{+2} and Zn^{+2}) in double distilled water at the different concentrations in this section. Figure 3 (a, b, c) shows that the determined resonance angles were 68.17˚, 67.39˚, 67.05˚ for Pb^{+2}, Cd^{+2}, Zn^{+2} at 100 ppm respectively. And the resonance angles are shifted to 68.99, 67.85˚, 67.82˚ at 1000 ppm for the above-mentioned metals, respectively.

From Fig 4, It is shown that I_{min} of Pb^{+2}, Cd^{+2} and Zn^{+2} solutions are decreased with increasing concentration from 100 to 1000 ppm for Pb^{+2}, Cd^{+2} and Zn^{+2} solutions. I_{min} decreased from Zn^{+2} to Cd^{+2} to Pb^{+2} respectively, this may be due to the difference in atomic weight of Zn^{+2} to Cd^{+2} to Pb^{+2}. Atomic weight of Pb^{+2} is higher than that of Cd^{+2} and Zn^{+2}. The red lines represent the curve fit to the experimental results for Pb^{+2}, Cd^{+2} and Zn^{+2} solutions. The following equations represent the fitting relations of Imin on the different solutions concentrations of metal ions (Pb^{+2}, $Cd^{+2}$and Zn^{+2}). Consequently I_{min}, can be determined for any concentration from the calibration curves, Fig 4. The curve fitting of I_{min} is listed in the following equations.

$$I_{min}Pb^{+2}=0.631+3.872E\text{-}5*C\text{-}9.649E\text{-}8*C^2 \quad (8.1)$$
$$I_{min}Cd^{+2}=0.642\text{-}7.692E\text{-}6*C\text{-}1.828E\text{-}8*C^2 \quad (8.2)$$
$$I_{min}Zn^{+2}=0.663\text{-}2.736E\text{-}5*C\text{-}1.004E\text{-}8*C^2 \quad (8.3)$$

From Fig.5, the maximum reflected intensity Imax (before the dip of the curve) of Pb^{+2}; Cd^{+2} and Zn^{+2} solutions are decreased with increasing concentration from 100 to 1000 ppm. The red lines represent the curve fit to the experimental data by the following equations.

$$IRmaxPb^{+2}=1.142\text{-}\ 4.335E\text{-}5*C+1.325\ E\text{-}8*C^2 \quad (9.1)$$
$$IRmaxCd^{+2}=1.180+1.192E\text{-}5*C\text{-}\ 5.712E\text{-}8*C^2 \quad (9.2)$$
$$IRmaxZn^{+2}=1.190\ –2.273E\text{-}5*C\text{-}\ 9.622E\text{-}9*C^2 \quad (9.3)$$

While Dependence of θ_{SPR} on the metal ions solutions were demonstrated in the Fig. 6. θ_{SPR} of Pb^{+2}, Cd^{+2} and Zn^{+2} solutions were shifted to higher values with increasing metal ion solutions with the same behavior but with different values. The plot also showed that the resonance angle is increased from Zn^{+2} to Cd^{+2} to Pb^{+2} respectively. This was mainly due to the increment number of ions absorbed to the metal surface. The change in the concentration of the samples (metal ion solutions) led to the change in the refractive indices on the surface of the metals which may be due to change in the resonance conditions. Fitting to data were extracted by the following equations.

$$\theta_{SPR}Pb^{+2}=68.305\text{–}8.926E\text{-}4*C+1.536E\text{-}6*C^2 \quad (10.1)$$
$$\theta_{SPR}Cd^{+2}=67.475\text{–}\ 4.719E\text{-}4*C+1.766E\text{-}6*C^2 \quad (10.2)$$
$$\theta_{SPR}Zn^{+2}=\ 67.111\text{–}\ 3.966E\text{-}4*C+1.104E\text{-}6*C \quad (10.3)$$

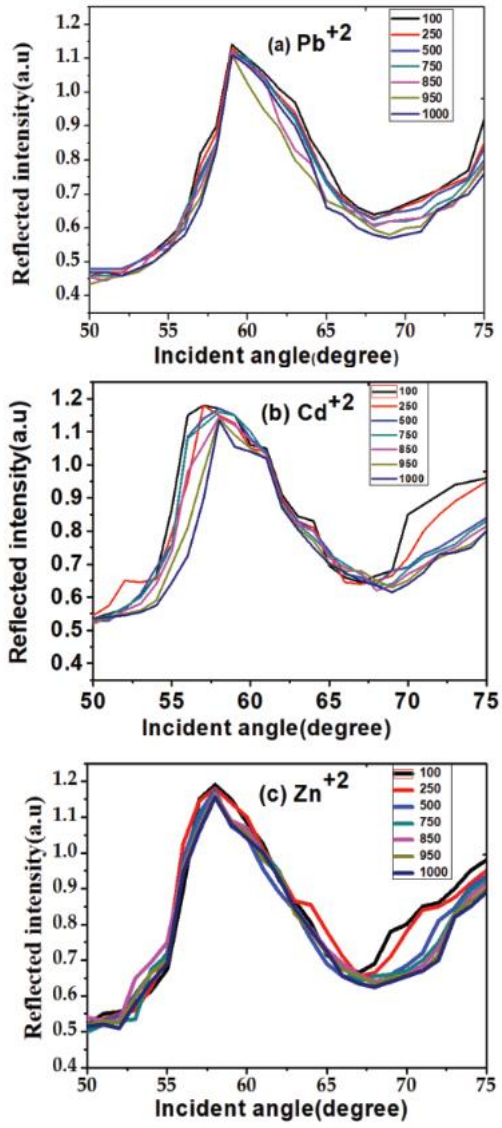

Fig. 3 SPR curves for metal ion solutions (a) Pb^{+2}, (b) Cd^{+2} and (c) Zn^{+2} at different concentrations.

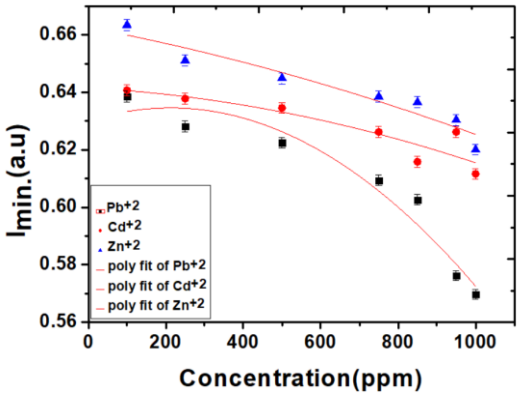

Fig. 4 The polynomial fitting of minimum reflected intensity (Imin) from SPR curves of Pb^{+2}, Cd^{+2} and Zn^{+2} solutions as a function of metal ion concentrations.

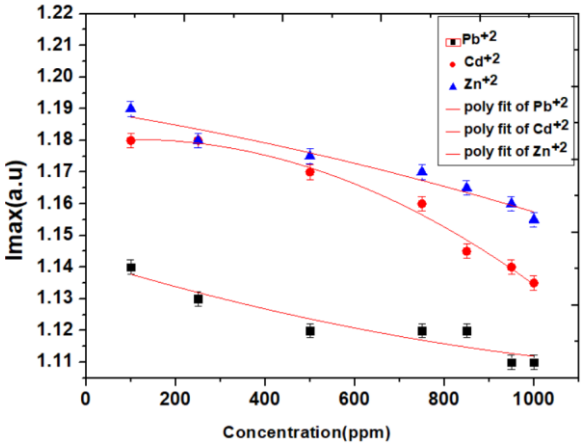

Fig. 5 The polynomial fitting of maximum reflected intensity (Imax) from SPR curve of Pb^{+2}, Cd^{+2} and Zn^{+2} solutions as a function of metal ions concentrations.

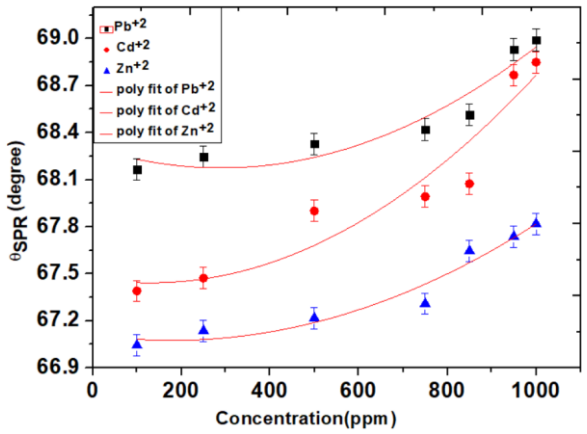

Fig. 6 The polynomial fitting of the resonance angle (θ_{SPR}) from SPR curve of Pb^{+2}, Cd^{+2} and Zn^{+2}solutions as a function of metal ions concentrations.

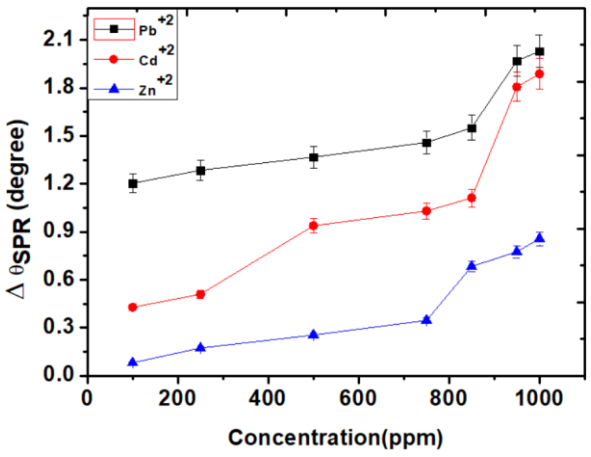

Fig. 7 θ_{SPR} shift of SPR curves of Pb^{+2}, Cd^{+2} and Zn^{+2} solutions from θ_{SPR} of double distilled water as a function of the concentrations of metal ions solutions.

Fig.7 shows that the shift in θ_{SPR} of Pb^{+2}, Cd^{+2} and Zn^{+2} increased with increasing concentrations. The shift in θ_{SPR} increased from Zn^{+2} to Cd^{+2} to Pb^{+2}respectively; this mainly might be due to the difference of atomic number of these metal ions based on periodic table as mentioned before. Kamaruddin et al [10] mentioned greater shift in SPR angle was observed with metals with higher values of electronegativity Pb^{2+} and Hg^{2+}. According to Pauling scale of electronegativity, the values of electronegativity of Pb, Cd, Zn are 2.33, 1.69 and 1.65 respectively. This confirmed our results were matched with the previous one and the shift of SPR resonance angle was increased with the increase of electronegativity of metals.

To conclude, SPR experiment was carried out for Pb^{+2}, Cd^{+2}, Zn^{+2} from 100 -1000 ppm, for lower concentration less than 100 ppm: the resonance angles remained unchanged from the resonance angle of double distilled water. No significant change in θ_{SPR} for concentrations in the range 0-100 ppm using equation (9). Fig.8 represents the calculation of θ_{SPR} in 0-100 ppm concentrations where these small changes in θ_{SPR} cannot be detected using the current configuration. This might be due to the lower sensor sensitivity. in addition to, small binding interaction to the gold film.

Fen et al [16] recorded similar unchanged in θ_{SPR} from 0.5 to 100 ppm, they attributed this issue a small number of ions existed to be adsorbed in the gold surface in these low concentrations. Danial et al reported no change in SPR resonance angle for Zn concentration (0.1-60 ppm) using the gold thin film which might be attributed to a small binding interaction amount of Zn^{+2} with the gold surface. [21] , hence they modified the gold layer with a nano-crystalline cellulose-based material to get better sensitivity. The goal of our current worked in progress is to improve the gold thin film with different materials as graphene to enhance the sensor sensitivity.

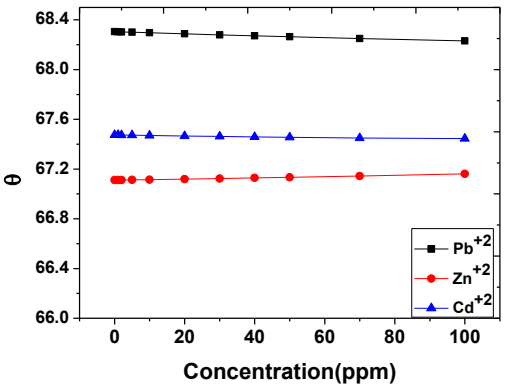

Fig. 8 Calculated θ_{SPR} in the range 0-100ppm according to the fitting equation 9

3.2 Real and imaginary parts of refractive indices of metal ion solutions at different concentrations calculated at λ = 632.8 nm

The real and imaginary parts of refractive index of Pb^{+2}, Cd^{+2} and Zn^{+2} are calculated analytically from resonance angle θ_{SPR} and complex refractive index of gold layer at wave length 632.8 nm in equation (3), The complex refractive index of gold layer (Au) at wave length 632.8 nm is 0.18377 - 3.4313i [22] , and the calculated refractive indices parts are represented as a function of concentration in Fig. 9. the real and the imaginary parts of refractive indices are increased with increasing the concentrations of Pb^{+2}, Cd^{+2} and Zn^{+2} solutions from 100 to 1000 ppm, this is due to with increasing metal ions concentrations in solutions, the resonance angle is shifted to a higher value so refractive index is increased. The real and imaginary parts of refractive indices are increased from Zn^{+2} to Cd^{+2} to Pb^{+2}, as θ_{SPR} of Pb^{+2}> θ_{SPR} Cd^{+2}> θ_{SPR} Zn^{+2}.

. 3.3 Performance of surface plasmon resonance detection

As mentioned in section 2.3, performance parameters were calculated as sensitivity, detection accuracy and the quality factor of the sensor. Based on spr curves analysis (fig.3) and calculation of the refractive indices, we extract the following parameters as tabled in table 1. $\Delta\theta$, Δn are the change of the SPR angle and the refractive index of metal ion solution with respect to the SPR angle of doubled distilled water. FWHM is the full width at half maximum of surface plasmon resonance angle.

Table 2 summarizes the calculated sensor parameters according to equations 4-6, we noticed a slight variation in the performance parameters for each metal solution, the higher sensitivity was found for Pb^{+2} metal ions, this may due to the higher electronegativity value of Pb^{+2}. The quality factor has the same range for all measured metal ions in contrast to Detection accuracy D.A of sensor values are increased for Pb^{+2} and Cd^{+2} more than that of Zn^{+2}.

Table 3 show a comparison of this work with others using sensing layers such as gold, silver, and bimetallic solver-gold film. the sensitivity of our sensing layers for Pb^{+2} was 124 deg./RIU. this is in a good agreement with other work in Table 3**.** The SPR sensor is simple and cost effective in comparisons to other metal detection techniques; however, the sensing is limited with angle modulation and the thickness of gold layer. Further improvement to the sensing probes is under investigation; our current work is building SPR sensor via wavelength modulation as optical fiber sensing[23], [24], [25].

Different conventional techniques have been established for sensing heavy metal ions in solution. These techniques consist of atomic absorption spectroscopy (AAS), inductively coupled plasma mass spectrometry (ICPMS), X-ray fluorescence spectrometry (XRF), anodic stripping voltammetry (ASV), and instrumental neutron activation

analysis (INAA). these techniques are listed in Table 4. AAS and ICPMS are destructive and high-cost devices. the other techniques such as XRD, ASV, and INAA are non-destructive techniques. however XRF needs long measuring time, while ASV has low detect limit and severe interference problems but in INAA , samples must be exposed to a neutron flux to produce radioactive nuclides.[26]

Table 5 represents the analytical performance of different analytical techniques for heavy metal ions detection. we calculated the limit of detection according to equation 7. we calculated the limit of detection, linearity, and relative standard deviation RSD. moreover, we compared it to different techniques such as dual electrochemical and colorimetric detection, ASV, XRF, and ICP-PS.

According to fig.7 the linearity range were found to be 100-850, 250-500, 100-750 ppm for Pb^{+2}, Cd^{+2}, Zn^{+2}, respectively. these ranges are corresponding to 0.3019-2.66, 0.8104-1.62, 0.336-2.5 mM for Pb^{+2}, Cd^{+2}, Zn^{+2} respectively.

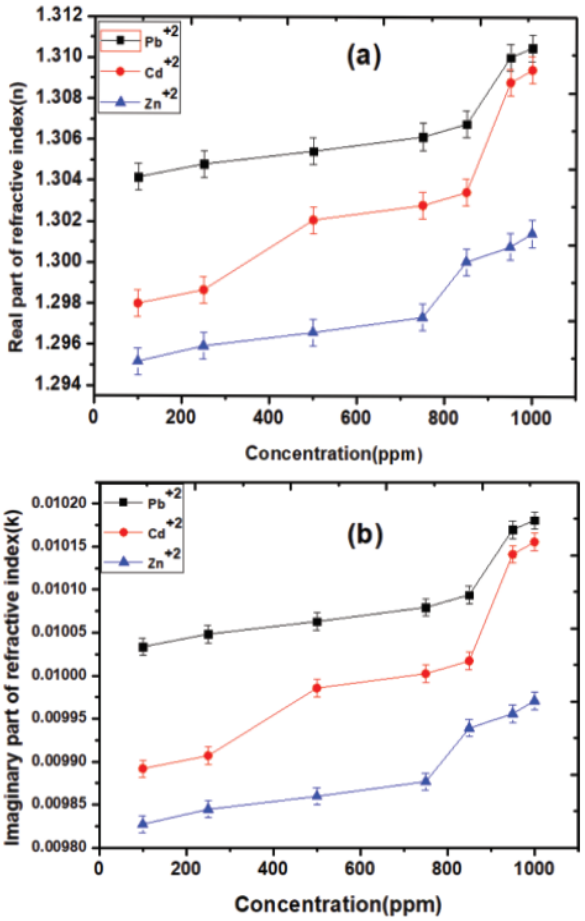

Fig. 9 (a) The real part of refractive index n, and (b) The imaginary part of refractive index k as a function of Pb^{+2}, $Cd^{+2}$and Zn^{+2} concentrations.

Table 1: The change in surfac plasmon resonance angle Δθ, Δn the change of refractive index of metal ions (with repect to distilled water), FWHM, I_{min} minum intensity for Pb^{+2}, Cd^{+2}, Zn^{+2} of different concentrations.

Metal conc.(ppm)	Δθspr			Δn			FWHM			I min		
	Pb^{+2}	Cd^{+2}	Zn^{+2}	Pb^{+2}	Cd^{+2}	Zn^{+2}	Pb^{+2}	Cd^{+2}	Zn^{+2}	Pb^{+2}	Cd^{+2}	Zn^{+2}
100	1.2058	0.43	0.0836	0.00968	0.00352	0.00069	11.07	10.04	11.58	0.6385	0.6407	0.6634
250	1.287	0.51	0.175	0.01032	0.00418	0.00144	9.26	11.67	11.66	0.6304	0.6378	0.6511
500	1.369	0.94	0.257	0.01095	0.0076	0.00211	9.43	12	12.61	0.6224	0.6346	0.6449
750	1.4608	1.03	0.34885	0.01166	0.00832	0.00286	9.45	12.34	12.01	0.6093	0.6262	0.6385
850	1.5425	1.11	0.6855	0.01229	0.00896	0.00557	11.65	12.51	12.35	0.6026	0.6158	0.6366
950	1.9709	1.81	0.777	0.01555	0.01431	0.0063	12.53	13.57	12.53	0.5762	0.6262	0.6304
1000	2.0309	1.89	0.8589	0.016	0.01493	0.00695	10.4671	13.7317	12.4361	0.5697	0.6116	0.62

Table 2 Calculated sensor performance parameters: Sensitivity (s), Detection Accuracy (D.A), and Quality factor (Q.F.)

	Sensitivity S			Detection Accuracy (D.A.)			Q.F		
Metal conc.(ppm)	Pb^{+2}	Cd^{+2}	Zn^{+2}	Pb^{+2}	Cd^{+2}	Zn^{+2}	Pb^{+2}	Cd^{+2}	Zn^{+2}

100	124.566116	122.15909	121.15942	0.1089	0.0428	0.0072	11.2526	12.1672	10.4628
250	124.709302	122.00957	121.52778	0.1390	0.0437	0.0150	13.4675	10.4550	10.4226
500	125.022831	123.68421	121.80095	0.1452	0.0783	0.0204	13.2580	10.3070	9.6591
750	125.283019	123.79808	121.97552	0.1546	0.0835	0.0290	13.2575	10.0323	10.1562
850	125.508544	123.88393	123.07002	0.1324	0.0887	0.0555	10.7733	9.9028	9.9652
950	126.745981	126.48498	123.33333	0.1573	0.1334	0.0620	10.1154	9.3209	9.8430
1000	126.93125	126.59076	123.58273	0.1940	0.1376	0.0691	12.1267	9.2189	9.9374

Table 3 a comparison of SPR sensors performance based Kretschmann configuration.

Sensing layers	Analyte	Real part of refractive index	Imaginary part of refractive index	Sensitivity	ref
gold	Cu^{+2}(100-1000ppm)	1.3321-1.3381	0.0042-0.0108		[27]
gold	Pb^{+2}(100-1000ppm)	1.3321-1.3388	0.0002-0.0086		[27]
gold	Pb^{+2}(0-100) ppm	1.3317-1.3321	0-0.0027		[16]
Ag film, low index prism		1.328–1.332	-	500 deg./RIU	[28]
Au and Si, ZrO2 thin film		1.325–1.335	-	50–230 deg./RIU	[29]
Bimetallic Ag-Au	Sucrose(0-5%wt)	1.33–1.34		7.85×10^{-6} RIU	[30]
Au, Ag metal film		1.33–1.34		100–300 deg./RIU	[31]
gold	Pb^{+2}(100-1000ppm)	1.304-1.312	0.0102-0.01018	124 deg./RIU	this work

Table 4: a comparison of spr techniques with other conventional techniques for heavy metal ions detections

Technique	**Detection range**	**Sensitivity**	**Destructive or not**	**Cost**	**measurement time**	**limitation**
atomic absorption spectroscopy (AAS)	Nanomolar range (nM)	High sensitivity	destructive	High cost	long measuring period	working at high temperatures (2,500-3,000^{0}C)
inductively coupled plasma mass spectrometry (ICPMS)	picomolar to nanomolar range (pM-nM)	Very high sensitivity	destructive	Very high cost		complicated sample pretreatment
X-ray fluorescence spectrometry (XRF)	nanomolar to micromolar (nM-**µ**M)	Good selectivity	non-destructive		long measuring period	High self-absorption of emitted radiation limiting the analysis of surface layers
anodic stripping voltammetry (ASV)	nanomolar range to micromolar (nM-**µ**M)	high sensitivity	non-destructive	low cost		Interferences problem
instrumental neutron activation analysis (INAA).	nanomolar to micromolar (nM-**µ**M)	High sensitivity and selectivity	non-destructive			needing nuclear irradiation
SPR spectroscopy	picomolar to micromolar (pM-**µ**M)	very high sensitivity	non-destructive	low cost	fast measurement	relatively low selectivity (improving)

Table 5 a Comparison of analytical performance of different analytical techniques for the determination of $Pb^{+2}Cd^{+2}$, and Zn^{+2}

Spr Kretschmann configuration	Pb^{+2}	0.00398	100-850 ppm	0.475	This work
	Cd^{+2}	0.00403	250-500 ppm	0.8371	
	Zn^{+2}	0.00403 (RIU)	100-750 ppm	0.4639	
dual electrochemical and colorimetric detection	Pb, Cd	0.1 ng/mL			[32]
ASV (microfabricated bismuth (Bi) electrode)	Pb^{+2},	8ppb	25-400 ppb		[33]

	Cd^{+2}	9.4 ppb	28-280 ppb		
ASV	Pb	0.3 $\mu g\ l^{-1}$	1-80 µg/L		[34]
ASV	Pb^{+2}	0.1 µg/L			[35]
	Cd^{+2}	0.1 µg/L			
	Zn^{+2}	1 µg/L			
XRF	Pb^{+2}	0.71 µg cm^{-2}			[36]
	Zn^{+2}	0.49 µg cm-2			
ICP–MS	Pb^{+2}	8.8 ng/L		7.4	[37]
	Cd^{+2}	1.7 ng/L		4.6	
AAS	Pb^{+2}	0.29 µg/L		4	
	Cd^{+2}	0.01 µg/L		2.22	[38]
	Zn^{+2}	0.994 µg/L		4.7	

Recent studies are reporting heavy metal ions detection via different techniques and innovative materials[39]–[41]. The role of using nanomaterial with the metallic film for spr enhancement is recently discussed in [42], where several nanoparticles such as gold and silver, magnetic nanoparticles , nanostructures based on graphene and graphene oxide can be applied. They reported the enhancement is due to the coupling between localized surface plasmon resonance LSPR of nanomaterial and the SPR of the metallic film which results in inducing a large electric field on the surface of the nanomaterial and consequently, there will be an increase in spr sensitivity. In our future work, We will fabricate new plasmonic materials for spr enhancement.

4 Conclusions

In this work, we built SPR sensor which is based Kretschmann setup. The sensor is used characterize various heavy metal ion solutions as Pb^{+2}, Cd^{+2} and Zn^{+2}. The resonance angle is shifted to higher values with increasing their content. The optical properties of metal ions solutions Pb^{+2}, Cd^{+2} and Zn^{+2} were calculated analytically using the resonance angle measurements. Both real and imaginary parts of refractive indices of heavy metal ions are increased with increasing concentration. (θ_{SPR}), (I_{min}) and (I_{max}) were determined for any concentration in the range of the calibration curves using the fitting equations for Pb^{+2}, Cd^{+2} and Zn^{+2} solutions. θ_{SPR}, I_{min} , and I_{max} were determined for any concentration in the range of the calibration curves using the fitting equations for Pb^{+2}, Cd^{+2} and Zn^{+2} solutions. The sensitivity, detection accuracy, and quality factor parameters of proposed SPR sensor were studied; these parameters show good quality of sensor measurements over different metal ions. The sensor is simple and has efficient cost among other sensing techniques. However, the setup is limited with angle modulation and the sensing layer of gold; the enhancement of SPR sensing layers via wavelength modulation is under study.

Conflicts of Interest: The authors declare no conflict of interest.

References

[1] J. Jana, M. Ganguly, and T. Pal, "Enlightening surface plasmon resonance effect of metal nanoparticles for practical spectroscopic application," *RSC Adv.*, vol. 6, no. 89, pp. 86174–86211, 2016, doi: 10.1039/c6ra14173k.

[2] S. B. D. Borah, T. Bora, S. Baruah, and J. Dutta, "Heavy metal ion sensing in water using surface plasmon resonance of metallic nanostructures," *Groundw. Sustain. Dev.*, vol. 1, no. 1–2, pp. 1–11, 2015, doi: 10.1016/j.gsd.2015.12.004.

[3] M. Mahmoudpour, J. Ezzati Nazhad Dolatabadi, M. Torbati, and A. Homayouni-Rad, "Nanomaterials based surface plasmon resonance signal enhancement for detection of environmental pollutions," *Biosens. Bioelectron.*, vol. 127, no. November 2018, pp. 72–84, 2019, doi: 10.1016/j.bios.2018.12.023.

[4] S. Mohammadzadeh-Asl, A. Keshtkar, J. Ezzati Nazhad Dolatabadi, and M. de la Guardia, "Nanomaterials and phase sensitive based signal enhancment in surface plasmon resonance," *Biosens. Bioelectron.*, vol. 110, no. February, pp. 118–131, 2018, doi: 10.1016/j.bios.2018.03.051.

[5] S. Pidishety, N. K. Viswanathan, B. Optics, and A. Group, "Imaging surface plasmon resonance polarimeter."

[6] C. Lertvachirapaiboon, A. Baba, S. Ekgasit, K. Shinbo, K. Kato, and F. Kaneko, "Transmission surface plasmon resonance techniques and their potential biosensor applications," *Biosens. Bioelectron.*, vol. 99, no. July 2017, pp. 399–415, 2018, doi: 10.1016/j.bios.2017.07.069.

[7] L. C. Oliveira, E. U. K. Melcher, C. Thirstrup, A. M. N. Lima, C. S. Moreira, and H. F. Neff, "A surface plasmon resonance biosensor for angular and wavelength operation," in *2012 IEEE International Instrumentation and Measurement Technology Conference Proceedings*, 2012, pp. 1214–1219, doi: 10.1109/I2MTC.2012.6229418.

[8] Y. M. Espinosa-Sánchez, D. Luna-Moreno, M. Rodríguez-Delgado, and A. Sánchez-Álvarez, "Determination of optical parameters of organic and inorganic thin films using both surface plasmon resonance and Abelès-Brewster methods," *Optik (Stuttg).*, vol. 142, pp. 426–435, 2017, doi: 10.1016/j.ijleo.2017.05.090.

[9] F.-C. Chien and S.-J. Chen, "A sensitivity comparison of optical biosensors based on four different surface plasmon resonance modes," *Biosens. Bioelectron.*, vol. 20, no. 3, pp. 633–642, Oct. 2004, doi: 10.1016/J.BIOS.2004.03.014.

[10] N. H. Kamaruddin, A. A. A. Bakar, N. N. Mobarak, M. S. Dzulkefly Zan, and N. Arsad, "Binding affinity of a highly sensitive Au/Ag/Au/Chitosan-graphene oxide sensor based on direct detection of Pb2+ and Hg2+ ions," *Sensors (Switzerland)*, vol. 17, no. 10, 2017, doi: 10.3390/s17102277.

[11] A. Patnaik, K. Senthilnathan, and R. Jha, "Graphene-Based Conducting Metal Oxide Coated D-Shaped Optical Fiber SPR Sensor," *IEEE Photonics Technol. Lett.*, vol. 27, no. 23, pp. 2437–2440, 2015, doi: 10.1109/LPT.2015.2467189.

[12] Y. Liu, Q. Liu, S. Chen, F. Cheng, H. Wang, and W. Peng, "Surface plasmon resonance biosensor based on smart phone platforms," *Sci. Rep.*, vol. 5, pp. 1–9, 2015, doi: 10.1038/srep12864.

[13] M. N. Hossen, M. Ferdous, M. Abdul Khalek, S. Chakma, B. K. Paul, and K. Ahmed, "Design and analysis of biosensor based on surface plasmon resonance," *Sens. Bio-Sensing Res.*, vol. 21, no. August, pp. 1–6, 2018, doi: 10.1016/j.sbsr.2018.08.003.

[14] X. Wang, S. Zhan, Z. Huang, and X. Hong, "REVIEW: ADVANCES AND APPLICATIONS OF SURFACE PLASMON RESONANCE BIOSENSING INSTRUMENTATION," *Instrum. Sci. Technol.*, vol. 41, no. 6, pp. 574–607, Nov. 2013, doi: 10.1080/10739149.2013.807822.

[15] S. Fajardo, García-Galvan, F. R., V. Barranco, J. C. Galvan, and S. F. Batlle, "We are IntechOpen , the world ' s leading publisher of Open Access books Built by scientists , for scientists TOP 1 %," *Intech*, vol. i, no. tourism, p. 13, 2016, doi: http://dx.doi.org/10.5772/57353.

[16] Y. W. Fen, W. M. M. Yunus, and Z. A. Talib, "Analysis of Pb(II) ion sensing by crosslinked chitosan thin film using surface plasmon resonance spectroscopy," *Optik (Stuttg).*, vol. 124, no. 2, pp. 126–133, 2013, doi: 10.1016/j.ijleo.2011.11.035.

[17] P. Length, "2. Surface Plasmons on Smooth Surfaces 2.1 Fundamental Properties: Dispersion Relation, Extension and Propagation Length for the Electromagnetic Fields of the Surface Plasmons Dispersion Relation."

[18] A. R. Sadrolhosseini, M. M. Moksin, H. L. L. Nang, M. Norozi, M. M. W. Yunus, and A. Zakaria, "Physical properties of normal grade biodiesel and winter grade biodiesel," *Int. J. Mol. Sci.*, vol. 12, no. 4, pp. 2100–2111, 2011, doi: 10.3390/ijms12042100.

[19] E. Kretschmann, "Die Bestimmung optischer Konstanten von Metallen durch Anregung von Oberflächenplasmaschwingungen," *Zeitschrift für Phys. A Hadron. Nucl.*, vol. 241, no. 4, pp. 313–324, Aug. 1971, doi: 10.1007/BF01395428.

[20] J. B. Maurya, Y. K. Prajapati, V. Singh, J. P. Saini, and R. Tripathi, "Improved performance of the surface plasmon resonance biosensor based on graphene or MoS2 using silicon," *Opt. Commun.*, vol. 359, pp. 426–434, Jan. 2016, doi: 10.1016/J.OPTCOM.2015.10.010.

[21] W. M. E. M. M. Daniyal *et al.*, "Enhancing the sensitivity of a surface plasmon resonance-based optical sensor for zinc ion detection by the modification of a gold thin film," *RSC Adv.*, vol. 9, no. 71, pp. 41729–41736, 2019, doi: 10.1039/c9ra07368j.

[22] P. B. Johnson and R. W. Christy, "Optical Constants of the Noble Metals," *Phys. Rev. B*, vol. 6, no. 12, pp. 4370–4379, Dec. 1972, doi: 10.1103/PhysRevB.6.4370.

[23] W. Liu, Z. Liu, Y. Zhang, S. Li, Y. Zhang, and X. Yang, "Specialty optical fibers and 2D materials for sensitivity enhancement of fiber optic SPR sensors : A review," *Opt. Laser Technol.*, vol. 152, no. March, p. 108167, 2022, doi: 10.1016/j.optlastec.2022.108167.

[24] R. Tabassum and R. Kant, "Recent trends in surface plasmon resonance based fiber–optic gas

sensors utilizing metal oxides and carbon nanomaterials as functional entities," *Sensors Actuators, B Chem.*, vol. 310, no. January, p. 127813, 2020, doi: 10.1016/j.snb.2020.127813.

[25] M. Gomaa, A. Salah, and G. Abdel Fattah, "Utilizing dip-coated graphene/nanogold to enhance SPR-based fiber optic sensor," *Appl. Phys. A*, vol. 128, no. 1, p. 56, Jan. 2022, doi: 10.1007/s00339-021-05196-z.

[26] Y. W. Fen and W. M. M. Yunus, "Surface plasmon resonance spectroscopy as an alternative for sensing heavy metal ions: A review," *Sens. Rev.*, vol. 33, no. 4, pp. 305–314, 2013, doi: 10.1108/SR-01-2012-604.

[27] Y. W. Fen and W. M. M. Yunus, "Characterization of the Optical Properties of Heavy Metal Ions Using Surface Plasmon Resonance Technique," *Opt. Photonics J.*, vol. 01, no. 03, pp. 116–123, 2011, doi: 10.4236/opj.2011.13020.

[28] D.-W. Huang, "Approach the angular sensitivity limit in surface plasmon resonance sensors with low index prism and large resonant angle," *Opt. Eng.*, vol. 49, no. 5, p. 054403, May 2010, doi: 10.1117/1.3431662.

[29] A. Lahav, M. Auslender, and I. Abdulhalim, "Sensitivity enhancement of guided-wave surface-plasmon resonance sensors," *Opt. Lett.*, vol. 33, no. 21, pp. 2539–2541, Nov. 2008, doi: 10.1364/OL.33.002539.

[30] K.-S. Lee, J. M. Son, D.-Y. Jeong, T. S. Lee, and W. M. Kim, "Resolution Enhancement in Surface Plasmon Resonance Sensor Based on Waveguide Coupled Mode by Combining a Bimetallic Approach," *Sensors*, vol. 10, no. 12, pp. 11390–11399, 2010, doi: 10.3390/s101211390.

[31] S. Roh, T. Chung, and B. Lee, "Overview of plasmonic sensors and their design methods," in *Advanced Sensor Systems and Applications IV*, 2010, vol. 7853, pp. 25–36, doi: 10.1117/12.869357.

[32] S. Chaiyo, A. Apiluk, W. Siangproh, and O. Chailapakul, "High sensitivity and specificity simultaneous determination of lead, cadmium and copper using μpAD with dual electrochemical and colorimetric detection," *Sensors Actuators, B Chem.*, vol. 233, pp. 540–549, 2016, doi: 10.1016/j.snb.2016.04.109.

[33] Z. Zou *et al.*, "Environmentally friendly disposable sensors with microfabricated on-chip planar bismuth electrode for in situ heavy metal ions measurement," *Sensors Actuators, B Chem.*, vol. 134, no. 1, pp. 18–24, 2008, doi: 10.1016/j.snb.2008.04.005.

[34] Y. Hong *et al.*, "Finite element modeling simulation-assisted design of integrated microfluidic chips for heavy metal ion stripping analysis," *J. Phys. D. Appl. Phys.*, vol. 50, no. 41, p. 415303, Oct. 2017, doi: 10.1088/1361-6463/aa84a3.

[35] N. Ruecha, N. Rodthongkum, D. M. Cate, J. Volckens, O. Chailapakul, and C. S. Henry, "Sensitive electrochemical sensor using a graphene–polyaniline nanocomposite for simultaneous detection of Zn(II), Cd(II), and Pb(II)," *Anal. Chim. Acta*, vol. 874, pp. 40–48, 2015, doi: https://doi.org/10.1016/j.aca.2015.02.064.

[36] Z. Chen, P. N. Williams, and H. Zhang, "Rapid and nondestructive measurement of labile Mn, Cu, Zn, Pb and As in DGT by using field portable-XRF," *Environ. Sci. Process. Impacts*, vol. 15, no. 9, pp. 1768–1774, 2013, doi: 10.1039/c3em00250k.

[37] N. Zhang, H. Peng, S. Wang, and B. Hu, "Fast and selective magnetic solid phase extraction of trace Cd, Mn and Pb in environmental and biological samples and their determination by ICP-MS," *Microchim. Acta*, vol. 175, no. 1–2, pp. 121–128, 2011, doi: 10.1007/s00604-011-0659-3.

[38] Ý. Kojuncu, J. M. Bundalevska, Ü. Ay, K. Cundeva, T. Stafilov, and G. Akçin, "Atomic absorption spectrometry determination of Cd, Cu, Fe, Ni, Pb, Zn, and T1 traces in seawater following flotation separation," *Sep. Sci. Technol.*, vol. 39, no. 11, pp. 2751–2765, 2004, doi: 10.1081/SS-200026751.

[39] M. M. Langari, M. M. Antxustegi, and J. Labidi, "Nanocellulose-based sensing platforms for heavy metal ions detection: A comprehensive review," *Chemosphere*, vol. 302, p. 134823, 2022, doi: https://doi.org/10.1016/j.chemosphere.2022.134823.

[40] X. Xu, S. Yang, Y. Wang, and K. Qian, "Nanomaterial-based sensors and strategies for heavy metal ion detection," *Green Anal. Chem.*, vol. 2, p. 100020, Aug. 2022, doi: 10.1016/j.greeac.2022.100020.

[41] A. Kumar Shakya and S. Singh, "State of the art in fiber optics sensors for heavy metals detection," *Opt. Laser Technol.*, vol. 153, p. 108246, Sep. 2022, doi: 10.1016/j.optlastec.2022.108246.

[42] A. Philip and A. R. Kumar, "The performance enhancement of surface plasmon resonance optical sensors using nanomaterials: A review," *Coord. Chem. Rev.*, vol. 458, p. 214424, May 2022, doi: 10.1016/j.ccr.2022.214424.